Since January 2020 Elsevier has created a COVID-19 resource centre with free information in English and Mandarin on the novel coronavirus COVID-19. The COVID-19 resource centre is hosted on Elsevier Connect, the company's public news and information website.

J. Comp. Path. 2008, Vol. 138, 171–179

Available online at www.sciencedirect.com

ScienceDirect

ELSEVIER
www.elsevier.com/locate/jcpa

Pathological Changes in Masked Palm Civets Experimentally Infected by Severe Acute Respiratory Syndrome (SARS) Coronavirus

Y. Xiao[*,†], Q. Meng[*,†], X. Yin[*], Y. Guan[*], Y. Liu[*], C. Li[*], M. Wang[*], G. Liu[*,†], T. Tong[*,†], L.-F. Wang[‡], X. Kong[*,†] and D. Wu[*,†]

[*] *National Key Laboratory of Veterinary Biotechnology, Harbin Veterinary Research Institute of the Chinese Academy of Agricultural Sciences (CAAS), Harbin 150001, China,* [†] *Graduate School of CAAS, Beijing 100081, China and* [‡] *CSIRO Livestock Industries, Australian Animal Health Laboratory, Australian Biosecurity Cooperative Research Centre for Emerging Infectious Diseases, Geelong, Victoria 3220, Australia*

Summary

Masked palm civets are highly susceptible to infection with the severe acute respiratory syndrome coronavirus (SARS-CoV). Infected animals become less aggressive and develop pyrexia, lethargy and diarrhoea. The present study describes the spectrum of histopathological changes in the lung, spleen, lymph node, liver, small intestine, kidney and cerebrum of civets infected experimentally with SARS-CoV. In-situ hybridization (ISH) with probes specific for the RNA polymerase gene demonstrated viral RNA in the lung, small intestine and cerebrum only. In-situ labelling was employed in order to demonstrate cellular apoptosis in the cerebrum, but there was no evidence of apoptosis within the myocardium. These results indicate that SARS-CoV causes multi-organ pathology in civets, similar to that observed in human SARS patients. These parallels suggest that civets may be used as an animal model of this infection to gain insight into the pathogenesis of SARS and for evaluation of candidate vaccines and antiviral drugs.

Keywords: apoptosis; civet; in-situ hybridization; SARS coronavirus

Introduction

Severe acute respiratory syndrome (SARS) first emerged in Guangdong Province in the People's Republic of China in November 2002. The aetiological agent of this syndrome was a newly emerged and previously unrecognized coronavirus, now known as SARS coronavirus (SARS-CoV) (Kuiken *et al.*, 2003; Ksiazek *et al.*, 2003). SARS is an acute pulmonary syndrome characterized by atypical pneumonia, progressive respiratory failure and death in up to 10% of infected individuals (Poon *et al.*, 2004). Although the SARS epidemic has subsided, many authorities, including the World Health Organization (WHO) and the US Centers for Disease Control and Prevention (CDC), have warned of the possible re-emergence of this highly infectious disease. It is therefore imperative that effective measures to prevent and treat the disease are developed and evaluated. To achieve this goal, animal models will play an essential role in studying the pathogenesis of SARS-CoV infection and in developing effective vaccines and therapeutics.

A wide range of animal species has been confirmed to be susceptible to experimental infection with SARS-CoV, including rodents (mice and hamsters), carnivores (ferrets and cats) and non-human primates (Wang *et al.*, 2006). Adult mice infected with SARS-CoV *via* the respiratory tract show no clinical signs of disease and only mild respiratory tract inflammation (Subbarao *et al.*, 2004). Aged mice, hamsters and ferrets do show signs of clinical disease such as weight loss and ruffled fur but do not develop lung pathology (Martina *et al.*, 2003; Roberts *et al.*, 2005a,b). Two groups of investigators have studied SARS-CoV

Correspondence to: X. Kong (e-mail: xgkong@hvri.ac.cn (X.K.), dlwu@hvri.ac.cn (D.W.)).

0021-9975/$ - see front matter
doi:10.1016/j.jcpa.2007.12.005

infection in African green monkeys and common marmosets (Kuiken *et al.*, 2003; McAuliffe *et al.*, 2004; Greenough *et al.*, 2005). Others have evaluated cynomolgus monkeys and rhesus macaques as potential models, but clinical disease is inconsistently induced in these latter species (Kuiken *et al.*, 2003; McAuliffe *et al.*, 2004; Rowe *et al.*, 2004).

Our laboratory has evaluated the suitability of guinea-pigs, hamsters, albino hamsters, chickens and rats as experimental models following inoculation of SARS-CoV strain BJ01. No clinical signs or tissue histopathological changes were observed in any of these animals post-infection. By contrast, all cynomolgus monkeys and rhesus macaques inoculated in this manner developed interstitial pneumonia of variable severity but no other tissue changes (Liu *et al.*, 2004). This pulmonary pathology was similar in nature to that seen in SARS patients, but the lesions were less severe than in infected humans. Therefore, there remains a requirement for an animal model of human SARS that closer approximates the tissue pathology that occurs in the human disease.

In October 2003 it was reported that SARS-CoV-like viruses had been isolated from masked palm civets from a live animal market in Guangdong, China (Guan *et al.*, 2003). This report prompted us to examine the feasibility of using civets as a better animal model for SARS. In a preliminary infection study, two groups of civets were inoculated with two different strains of SARS-CoV. Strain GZ01 was isolated during the early stages of the SARS epidemic and strain BJ01 was isolated during the middle phase of the epidemic (Wu *et al.*, 2005). Both strains were shown capable of infecting civets and inducing clinical signs including pyrexia, lethargy and loss of aggression (Wu *et al.*, 2005). The aim of the present study was to extend these observations by characterizing the tissue pathology in the infected civets and determining the distribution of viral RNA in tissues from those animals. In addition, analysis of cellular apoptosis in selected tissues was also conducted in an attempt to understand the pathogenesis of this viral infection in civets and to further determine the suitability of this species to model the human disease.

Materials and Methods

Virus, Animals and Inoculation

The animals and groups used in this study correspond exactly to those described in a previous publication (Wu *et al.*, 2005). SARS-CoV isolates were propagated in Vero E6 cells for two additional passages to generate virus stocks with titres of 1×10^6 50% tissue culture infective doses ($TCID_{50}$)/ml. Ten one-year-old masked palm civets were housed in individual biosafety isolators and were divided into two groups ($n = 5$ per group). Animals in groups A and B were inoculated with 3 ml of virus solution containing 3×10^6 $TCID_{50}$ of BJ01 and GZ01 isolates, respectively, with 2 ml instilled into the trachea and 1 ml given intranasally. A control civet was mock-infected in an identical fashion with 3 ml of Vero E6 cell culture supernatant. All work with infectious virus was performed inside a biosafety cabinet, in an approved animal biosafety level 3 laboratory. Serology and polymerase chain reaction (PCR) analysis were conducted to confirm that the civets had not been previously exposed to SARS-CoV. Animal experiments were conducted in accordance with the animal ethics guidelines and approved protocols issued by the Harbin Veterinary Research Institute, Chinese Academy of Agricultural Sciences.

Histopathology

One animal from each group was sacrificed at 3, 13, 23, 34 and 35 days post-infection (dpi), and lung, spleen, lymph node, small intestine, kidney, trachea, cerebrum, pancreas, sex glands, stomach and heart were collected from each animal. These samples were fixed in 10% neutral buffered formalin and embedded in paraffin wax. Sections taken from these blocked samples were stained by haematoxylin and eosin (HE).

In-situ Hybridization (ISH)

Two 3-digoxigenin-labelled oligonucleotide probes (Probe 1: 5′-acc ctg cta aag cat ata agg att acc tag-3′; Probe 2: 5′-CAA TGG CTG ATT TAG TCT ATG CTC TAC GTC-3′), which target the RNA polymerase gene of SARS-CoV, were purchased from Invitrogen (Carlsbad, California, USA). ISH was performed on the full range of tissues collected from each animal with ready-to-use reagents purchased from Boster Biological Technology Co. Ltd. (Wuhan, China) following the manufacturer's instructions. Briefly, tissue sections were de-waxed in xylene and rehydrated in gradient ethanol. Endogenous peroxidase activity was quenched by incubation in 3% H_2O_2. The tissues were digested with 3 mg/ml pepsin in 0.14 M citric acid at 37°C for 20 min and incubated at 37°C for 4 h with pre-hybridization buffer containing 35% deionized formamide, 5 × standard saline citrate, 2% blocking reagent, 0.1% *N*-lauroylsarcosine, 0.02% sodium dodecyl sulphate and 100 ng/ml salmon sperm DNA. The tissue sections were hybridized with digoxigenin-labelled

oligonucleotide probes (10 μg/ml) at 37°C for 18 h. The slides were rinsed in a series of graded salt solutions (×2, ×0.5 and ×0.2 standard saline citrate). After blocking at 37°C for 30 min, the sections were incubated with biotin-labelled mouse anti-digoxigenin antibody at 37°C for 60 min, followed by incubation with avidin-peroxidase conjugate at 37°C for 20 min. The signals were developed using the substrate diaminobenzidine tetrahydrochloride (DAB) and slides were counterstained with Mayer's haematoxylin. The same organs from the uninfected control civet were used as negative controls.

Detection of Apoptosis

Cerebrum and heart from all infected animals and one uninfected control animal were used for detection of cellular apoptosis. Apoptotic cells were identified using an in-situ cell apoptosis detection kit (Boster Biological Technology Co. Ltd.) according to the manufacturer's instructions. Briefly, cerebral and cardiac tissues embedded in paraffin wax were de-waxed in xylene and rehydrated in gradient ethanol. Endogenous peroxidase activity was quenched in 3% H_2O_2 for 10 min. The sections were washed three times, 5 min for each wash, with Tris-buffered saline (TBS; 0.01 M Tris, 0.15 M NaCl, pH 7.4) after digestion with proteinase K. The sections were exposed to biotin-16-dUTP and terminal deoxynucleotidyl transferase in labelling buffer (1 in 10) at 37°C for 2 h, followed by the same washing process as described above. After blocking at 37°C for 30 min, the sections were incubated with anti-digoxigenin antibody and avidin-peroxidase conjugate, followed by signal development using identical procedures to those described above.

Results

Clinical Signs

As previously described (Wu *et al*., 2005), from 3 dpi, all infected animals became lethargic and less aggressive. Febrile episodes also commenced around 3 dpi and temperatures remained elevated for up to 7 days. Diarrhoea developed between 3 and 14 dpi in infected civets. Leucopenia was also observed, with white blood cell counts reaching a minimum at approximately 3 dpi and returning to normal from 13 dpi onwards. The uninfected control animal remained clinically normal throughout the experiment.

Pathological Changes

No gross pathological changes were observed in any of the infected animals or in the uninfected control animal. In comparison to the control animal, various histopathological changes were observed in civets infected with SARS-CoV and these were similar in the animals infected with the two different SARS-CoV isolates. The histopathological changes for different organs are summarized below.

Lungs. At 3 dpi, acute interstitial inflammatory infiltrates and oedema were evident and there was congestion of the alveolar septae. The lumina of alveoli and bronchioles were variably filled with protein-rich oedema fluid, erythrocytes, cellular debris and lymphocytes (Fig. 1a). At 13 dpi, the pathological changes remained severe. The alveolar septae were thickened with infiltration of macrophages and lymphocytes and congestion of vessels (Fig. 1b). The lesions of interstitial pneumonia were even more distinct at 23 dpi, but by 34 and 35 dpi only foci of interstitial pneumonia remained.

Spleen. At 3 dpi there was extensive patchy necrosis of the splenic tissue, with atrophy of white pulp lymphoid aggregates (Fig. 1c). The atrophy of white pulp decreased in severity from 13 dpi but was still evident at 35 dpi.

Lymph Nodes. At 13 dpi there was depletion of lymphoid follicles within the lymph nodes (Fig. 1d) and this change was also observed at 23 dpi.

Liver. At 3 dpi there was diffuse congestion of the liver (Fig. 1e). Focal aggregations of lymphocytes were present in hepatic lobules and portal areas at days 13 and 23 dpi. At later time points there were no microscopical abnormalities in the liver.

Cerebrum. Within the cerebrum there was evidence of neuronal degeneration and mild neuronophagia from 3 to 13 dpi (Fig. 1f). In two cases there was mild oedema around the small veins and nerve cells. No microscopical changes were observed in this tissue after 13 dpi.

Kidneys. There was focal haemorrhage within the renal cortex at 3 dpi, but no changes were found after 23 dpi.

Small Intestine. Mild focal haemorrhage was observed in the lamina propria of the small intestine at 13 dpi.

Localization of Viral RNA

ISH was employed to locate SARS-CoV in tissue sections collected from infected civets. As expected, the tissue sections from organs of the control civet were negative for ISH. Positive signals were detected in

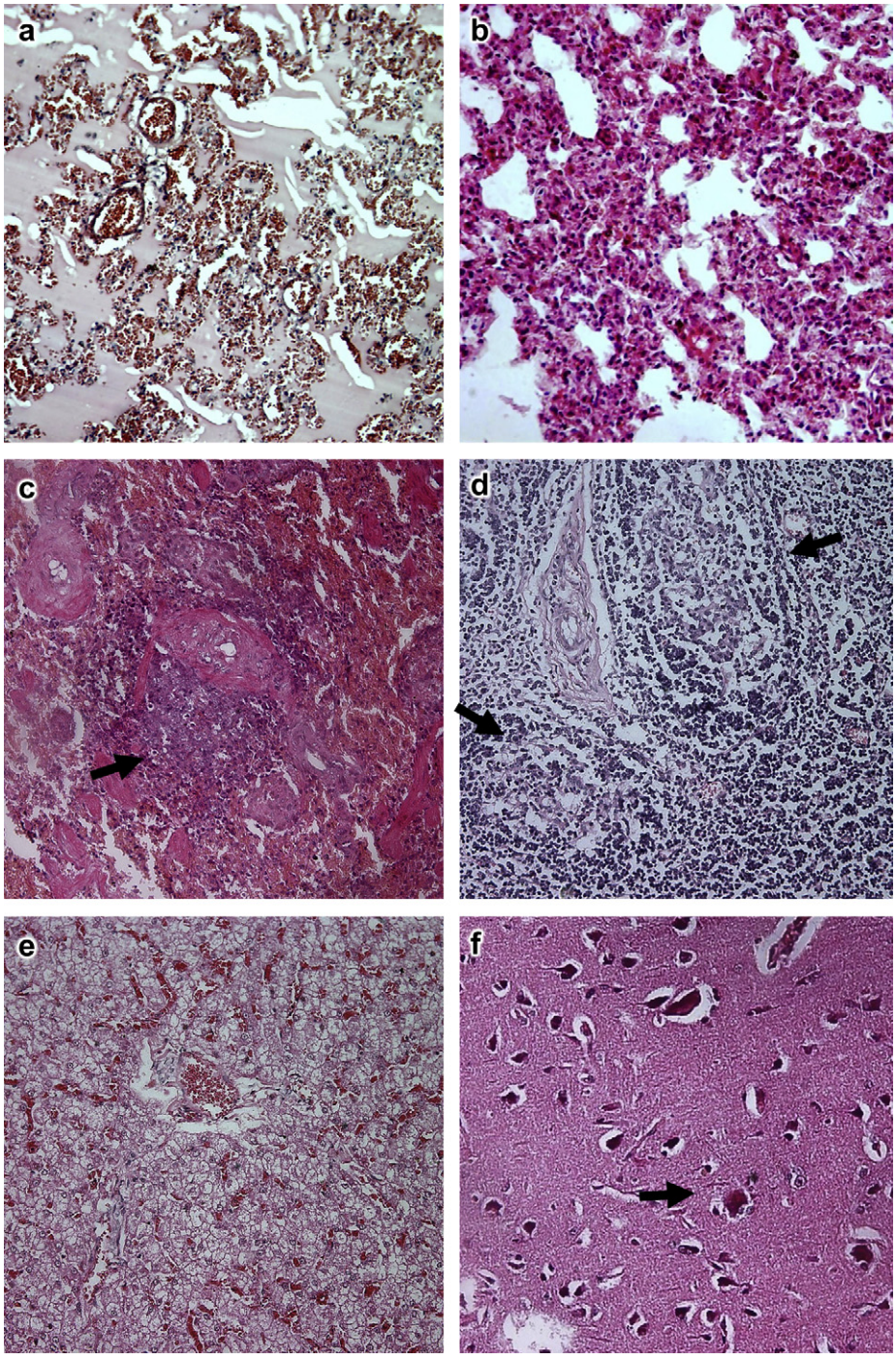

Fig. 1. Histopathological changes in infected civets. (a) Interstitial pneumonia at 3 dpi showing protein-rich oedema fluid in the lumina of bronchioles and alveoli. HE, ×200. (b) Interstitial pneumonia at 13 dpi. HE, ×400. (c) Atrophy of splenic lymphoid tissue (arrowed) at 3 dpi. HE, ×200. (d) Depletion of lymphoid follicles in lymph node (arrowed) at 13 dpi. HE, ×200. (e) Congestion and vacuolar degeneration of hepatocytes at 3 dpi. HE, ×100. (f) Neuronal degeneration and neuronophagia (arrowed) in cerebrum at 3 dpi. HE, ×400.

the lungs of infected animals at 3 dpi in both groups. In these animals SARS-CoV was also isolated by cell culture and the presence of viral RNA was confirmed by reverse transcriptase polymerase chain reaction (RT-PCR; Table 1 and Wu *et al.*, 2005). Positive signals were also found in the small intestine (3 dpi in both groups) and cerebrum (3 and 13 dpi in both groups).

Table 1
Detection of SARS-CoV and apoptosis in tissue from infected civets

Group (virus isolate)	*Days post-infection*	*Tissue examined*															
		Lung				*Heart*				*Cerebrum*				*Small intestine*			
		A	*B*	*C*	*D*	*A*	*B*	*C*	*D*	*A*	*B*	*C*	*D*	*A*	*B*	*C*	*D*
A (GZ01)	3	+	+	+	ND	–	–	–	–	ND	ND	+	+	ND	ND	+	ND
	13	–	–	–	ND	–	+	–	–	ND	ND	+	–	ND	ND	–	ND
	23	–	–	–	ND	–	–	–	–	ND	ND	–	–	ND	ND	–	ND
	34	–	–	–	ND	–	–	–	–	ND	ND	–	–	ND	ND	–	ND
	35	–	–	–	ND	–	–	–	–	ND	ND	–	–	ND	ND	–	ND
B (BJ01)	3	+	+	+	ND	+	+	–	–	ND	ND	+	+	ND	ND	+	ND
	13	–	–	–	ND	–	–	–	–	ND	ND	+	–	ND	ND	–	ND
	23	–	–	–	ND	–	–	–	–	ND	ND	–	–	ND	ND	–	ND
	34	–	–	–	ND	–	–	–	–	ND	ND	–	–	ND	ND	–	ND
	35	–	–	–	ND	–	–	–	–	ND	ND	–	–	ND	ND	–	ND

A, virus isolation; B, RT-PCR; C, ISH; D, apoptosis; (+), positive for virus isolation, PCR, ISH and apoptosis; (–), negative for virus isolation, PCR, ISH and apoptosis; ND, not determined.

These signals were localized to the cytoplasm of pneumocytes lining the alveolar septae and macrophages within the alveolar spaces (Fig. 2a). In the small intestine, the positive signal was mainly localized to macrophages (Fig. 2b). In the cerebrum, positive signals were mainly associated with glial cells at 3 dpi (Fig. 2c) and neurons at 13 dpi (Fig. 2d). No positive signal was found in any other tissue (Table 1).

Cellular Apoptosis

At 3 dpi, glial cells of the cerebrum in both groups of infected animals underwent apoptosis (Fig. 3a) and at 13 dpi there was also evidence of neuronal apoptosis (Fig. 3b). No apoptosis was noted in the myocardium at 3 dpi. By 13 dpi, no apoptosis was found either in the myocardium or in the cerebrum (Table 1).

Discussion

The causative agent of SARS has been identified as a new coronavirus not previously endemic in humans (Kuiken *et al*., 2003). This finding is supported by the lack of serological evidence of previous infection in healthy humans, which suggests that SARS-CoV has recently emerged in the human population. It has been proposed that animal-to-human interspecies transmission is the most probable explanation for emergence of the SARS-CoV. Recent epidemiological investigations by two independent groups suggest that bats may be a natural reservoir of SARS-CoV. Bats are among the live animals sold in markets in southern China, providing a possible explanation for the occurrence of infection among civets and other animals in these markets (Lau *et al*., 2005; Li *et al*., 2005a).

The isolation of SARS-CoV from palm civets was a significant finding in identifying this species as a source of the human SARS-CoV, but its role as a potential natural reservoir has not been established (Guan *et al*., 2003). In one study it was shown that SARS-CoV genome sequences from civets underwent rapid evolution before transmission to humans, suggesting that civets were a relatively new host to those viruses, rather than a natural reservoir host that had adapted to SARS-CoV (Song *et al*., 2005). In another study it was shown that while approximately 80% of civets in one market in Guangzhou had serological evidence of infection by SARS-CoV, animals on farms were largely free from infection. This suggested that infection of civets was associated with trading activities under conditions of overcrowding and mixing of various animal species, which provided an environment for efficient interspecies transmission (Tu *et al*., 2004). Furthermore, it has been shown that the S proteins of SARS-CoV isolated from human patients in the early stage of the outbreaks bound to and utilized the civet ACE2 receptor molecule, but S proteins of the civet isolates used human ACE2 markedly less efficiently (Li *et al*., 2005b). These findings provide evidence that civets have served as an efficient amplification host for SARS-CoV and that the SARS-CoV has undergone rapid evolution after transmission to the human population.

While it is now commonly believed that civets are unlikely to be the natural reservoir of SARS-CoV, the high susceptibility of this species to infection and the efficient amplification of SARS-CoV during the SARS outbreaks remain focal points for further investigation. It is important to know why civets display higher susceptibility to infection by SARS-CoV in

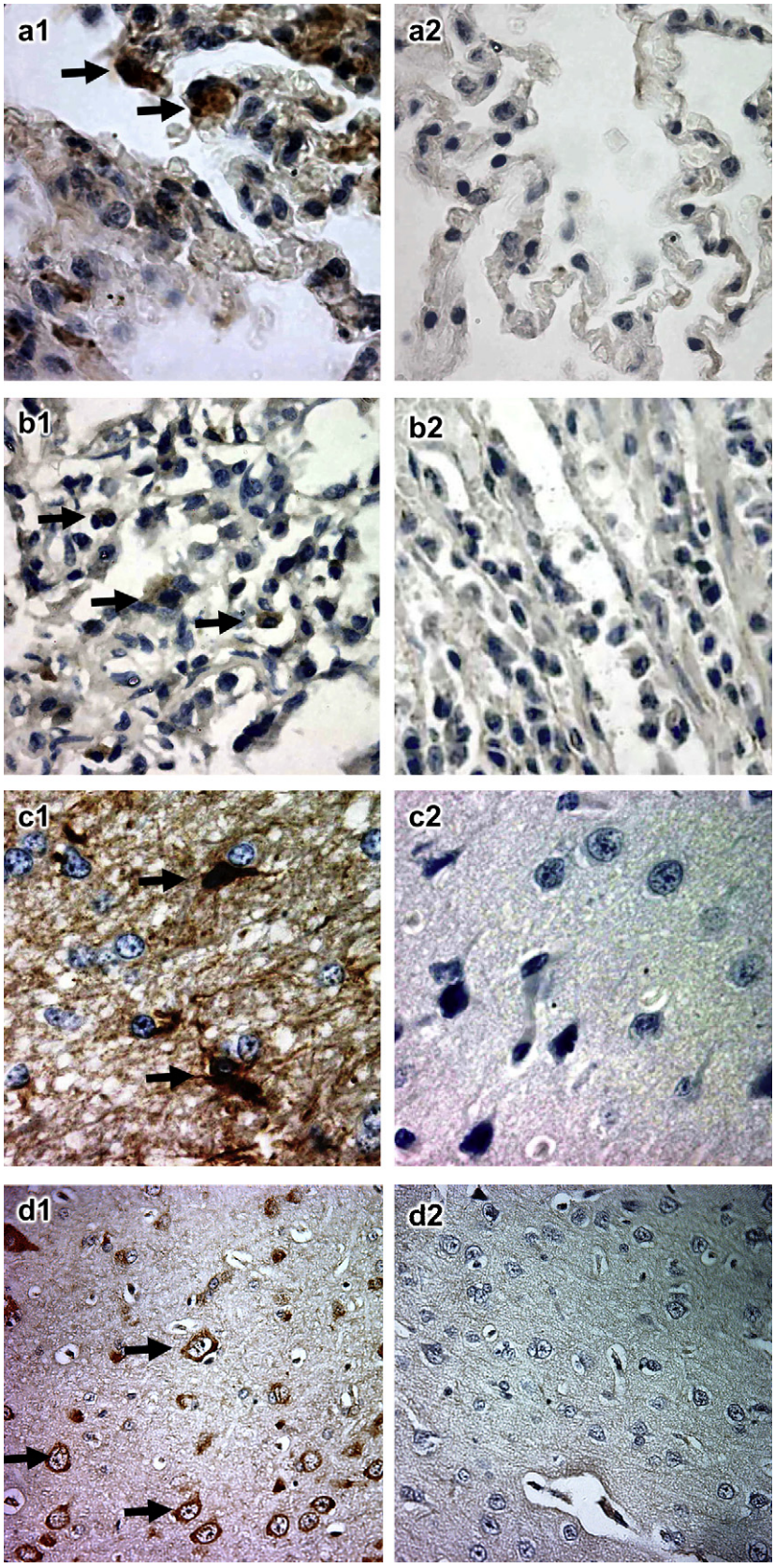

Fig. 2. Detection of SARS-CoV RNA by ISH. For each tissue tested, the left panel shows the result for infected civets whereas the right panel shows the non-infected control. (a) Lung showing labelling of macrophages (arrowed). (b) Small intestine showing labelling of macrophages (arrowed). (c) Glial cells of cerebrum (arrowed). (d) Neuron within the cerebrum (arrowed). (a)–(c), ×1000; (d), ×400.

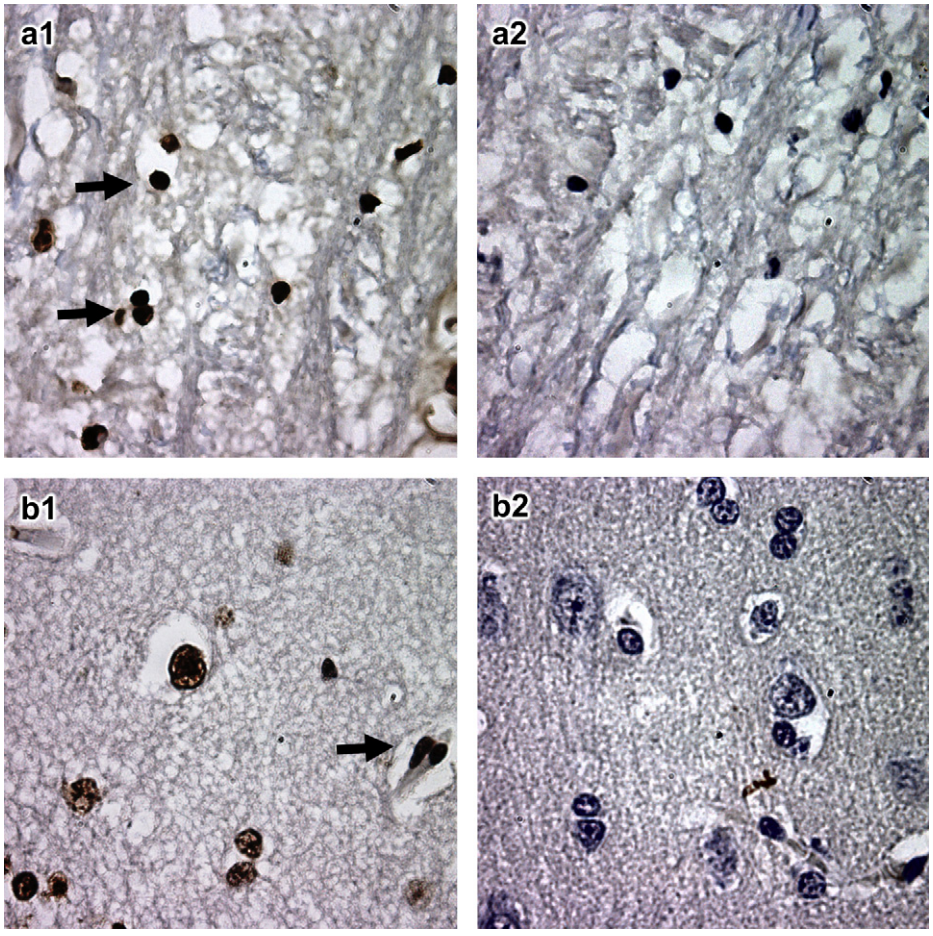

Fig. 3. Detection of apoptosis in cerebrum. The left panel shows the result for infected civets, whereas the right panel shows the non-infected control. (a) Neuron and (b) glial cells. Arrows indicate cells undergoing apoptosis, ×1000.

the market environment and whether civets have similar clinical and pathological changes as humans post-infection.

In the present study, multi-organ pathological changes were found in experimentally infected civets. The lungs were the main target organs, but changes were also identified within the spleen, lymph node, cerebrum, liver, kidney and small intestine. Interstitial pneumonia and diffuse alveolar damage were observed in lungs throughout the experiment. These lesions were similar to those described for SARS-CoV-infected macaques (Fouchier *et al*., 2003; Kuiken *et al*., 2003; Qin *et al*., 2005), but were milder than in humans with SARS (Ding *et al*., 2003; Franks *et al*., 2003; Nicholls *et al*., 2003; Tse *et al*., 2004). The observed follicular depletion in lymph nodes and atrophy of splenic white pulp also occur in human SARS (Zhao *et al*., 2003).

We have also demonstrated the presence of SARS-CoV RNA in the cytoplasm of alveolar epithelia, macrophages infiltrating the pulmonary interstitium, macrophages of the small intestine and glial cells and neurons of the cerebrum. This distribution is again similar to that observed in human SARS patients (Ding *et al*., 2004; To *et al*., 2004; Nicholls *et al*., 2006). There is currently little information available regarding the distribution of SARS-CoV RNA in other experimental animals with the exception of detection of viral RNA in bronchiolar epithelial cells of mice at 2 dpi (Subbarao *et al*., 2004). In-situ apoptosis analysis revealed that for two civets, glial cells and neurons in the cerebrum displayed apoptosis at 3 and 13 dpi, respectively. This finding suggests that SARS-CoV may cause direct damage to those cells, providing useful information for future study of disease pathogenesis. The same set of probes and methods were applied to SARS-CoV infected monkey tissues obtained from previous studies, but no positive results were obtained, suggesting that civets and monkeys respond differently to SARS-CoV infection.

In summary, the data presented in this study further corroborate previous findings (Wu *et al*., 2005) in demonstrating that civets are more susceptible to SARS-CoV infection than other animals, as implied

by their clinical symptoms, pathological changes and virus distribution within tissues. These observations raise the possibility that civets may be a superior model for SARS-CoV infection when compared with other animals that have been studied to date.

Acknowledgments

We thank Qingyu Zhu of the Institute of Microbiology and Epidemiology, Academy of Military Medical Sciences, Beijing, China, for providing SARS-CoV isolates BJ01 and GZ01 and the Vero E6 cell line. This project was funded by a special grant for identifying the animal reservoir of the SARS-CoV-like virus (2003A02) from the Ministry of Science and Technology of China.

References

Ding, Y., He, L., Zhang, Q., Huang, Z., Che, X., Hou, J., Wang, H., Shen, H., Qiu, L. and Li, Z., et al. (2004). Organ distribution of severe acute respiratory syndrome (SARS) associated coronavirus (SARS-CoV) in SARS patients: implications for pathogenesis and virus transmission pathways. *Journal of Pathology*, **203**, 622–630.

Ding, Y., Wang, H., Shen, H., Li, Z., Geng, J., Han, H., Cai, J., Li, X., Kang, W. and Weng, D., et al. (2003). The clinical pathology of severe acute respiratory syndrome (SARS): a report from China. *Journal of Pathology*, **200**, 282–289.

Fouchier, R. A., Kuiken, T., Schutten, M., van Amerongen, G., van Doornum, G. J., van den Hoogen, B. G., Peiris, M., Lim, W., Stohr, K. and Osterhaus, A. D. (2003). Aetiology: Koch's postulates fulfilled for SARS virus. *Nature*, **423**, 240.

Franks, T. J., Chong, P. Y., Chui, P., Galvin, J. R., Lourens, R. M., Reid, A. H., Selbs, E., McEvoy, C. P., Hayden, C. D. and Fukuoka, J., et al. (2003). Lung pathology of severe acute respiratory syndrome (SARS): a study of 8 autopsy cases from Singapore. *Human Pathology*, **34**, 743–748.

Greenough, T. C., Carville, A., Coderre, J., Somasundaran, M., Sullivan, J. L., Luzuriaga, K. and Mansfield, K. (2005). Pneumonitis and multi-organ system disease in common marmosets (*Callithrix jacchus*) infected with the severe acute respiratory syndrome-associated coronavirus. *American Journal of Pathology*, **167**, 455–463.

Guan, Y., Zheng, B. J., He, Y. Q., Liu, X. L., Zhuang, Z. X., Cheung, C. L., Luo, S. W., Li, P. H., Zhang, L. J. and Guan, Y. J., et al. (2003). Isolation and characterization of viruses related to the SARS coronavirus from animals in southern China. *Science*, **302**, 276–278.

Ksiazek, T. G., Erdman, D., Goldsmith, C. S., Zaki, S. R., Peret, T., Emery, S., Tong, S., Urbani, C., Comer, J. A. and Lim, W., et al. (2003). A novel coronavirus associated with severe acute respiratory syndrome. *New England Journal of Medicine*, **348**, 1953–1966.

Kuiken, T., Fouchier, R. A., Schutten, M., Rimmelzwaan, G. F., van Amerongen, G., van Riel, D., Laman, J. D., de Jong, T., van Doornum, G. and Lim, W., et al. (2003). Newly discovered coronavirus as the primary cause of severe acute respiratory syndrome. *Lancet*, **362**, 263–270.

Lau, S. K., Woo, P. C., Li, K. S., Huang, Y., Tsoi, H. W., Wong, B. H., Wong, S. S., Leung, S. Y., Chan, K. H. and Yuen, K. Y. (2005). Severe acute respiratory syndrome coronavirus-like virus in Chinese horseshoe bats. *Proceedings of the National Academy of Sciences of the United States of America*, **102**, 14040–14045.

Li, W., Shi, Z., Yu, M., Ren, W., Smith, C., Epstein, J. H., Wang, H., Crameri, G., Hu, Z. and Zhang, H., et al. (2005a). Bats are natural reservoirs of SARS-like coronaviruses. *Science*, **310**, 676–679.

Li, W., Zhang, C., Sui, J., Kuhn, J. H., Moore, M. J., Luo, S., Wong, S. K., Huang, I. C., Xu, K. and Vasilieva, N., et al. (2005b). Receptor and viral determinants of SARS-coronavirus adaptation to human ACE2. *EMBO Journal*, **24**, 1634–1643.

Liu, B. H., Wu, D. L., Zhan, D. W., Qin, E. D., Zhu, Q. Y., Wang, C. E., Meng, Q. W., Peng, W. M., Yin, X. N. and Yang, Y. H., et al. (2004). Study on the animal model for severe acute respiratory syndrome. *Wei Sheng Wu Xue Bao*, **44**, 711–716.

Martina, B. E., Haagmans, B. L., Kuiken, T., Fouchier, R. A., Rimmelzwaan, G. F., Van Amerongen, G., Peiris, J. S., Lim, W. and Osterhaus, A. D. (2003). Virology: SARS virus infection of cats and ferrets. *Nature*, **425**, 915.

McAuliffe, J., Vogel, L., Roberts, A., Fahle, G., Fischer, S., Shieh, W. J., Butler, E., Zaki, S., St Claire, M., Murphy, B. and Subbarao, K. (2004). Replication of SARS coronavirus administered into the respiratory tract of African Green, rhesus and cynomolgus monkeys. *Virology*, **330**, 8–15.

Nicholls, J. M., Butany, J., Poon, L. L., Chan, K. H., Beh, S. L., Poutanen, S., Peiris, J. S. and Wong, M. (2006). Time course and cellular localization of SARS-CoV nucleoprotein and RNA in lungs from fatal cases of SARS. *PLoS Medicine*, **3**, e27.

Nicholls, J. M., Poon, L. L., Lee, K. C., Ng, W. F., Lai, S. T., Leung, C. Y., Chu, C. M., Hui, P. K., Mak, K. L. and Lim, W., et al. (2003). Lung pathology of fatal severe acute respiratory syndrome. *Lancet*, **361**, 1773–1778.

Poon, L. L., Guan, Y., Nicholls, J. M., Yuen, K. Y. and Peiris, J. S. (2004). The aetiology, origins, and diagnosis of severe acute respiratory syndrome. *Lancet Infectious Diseases*, **4**, 663–671.

Qin, C., Wang, J., Wei, Q., She, M., Marasco, W. A., Jiang, H., Tu, X., Zhu, H., Ren, L. and Gao, H., et al. (2005). An animal model of SARS produced by infection of *Macaca mulatta* with SARS coronavirus. *Journal of Pathology*, **206**, 251–259.

Roberts, A., Paddock, C., Vogel, L., Butler, E., Zaki, S. and Subbarao, K. (2005a). Aged BALB/c mice as

a model for increased severity of severe acute respiratory syndrome in elderly humans. *Journal of Virology*, **79**, 5833–5838.

Roberts, A., Vogel, L., Guarner, J., Hayes, N., Murphy, B., Zaki, S. and Subbarao, K. (2005b). Severe acute respiratory syndrome coronavirus infection of golden Syrian hamsters. *Journal of Virology*, **79**, 503–511.

Rowe, T., Gao, G., Hogan, R. J., Crystal, R. G., Voss, T. G., Grant, R. L., Bell, P., Kobinger, G. P., Wivel, N. A. and Wilson, J. M. (2004). Macaque model for severe acute respiratory syndrome. *Journal of Virology*, **78**, 11401–11404.

Song, H. D., Tu, C. C., Zhang, G. W., Wang, S. Y., Zheng, K., Lei, L. C., Chen, Q. X., Gao, Y. W., Zhou, H. Q. and Xiang, H., et al. (2005). Cross-host evolution of severe acute respiratory syndrome coronavirus in palm civet and human. *Proceedings of the National Academy of Sciences of the United States of America*, **102**, 2430–2435.

Subbarao, K., McAuliffe, J., Vogel, L., Fahle, G., Fischer, S., Tatti, K., Packard, M., Shieh, W. J., Zaki, S. and Murphy, B. (2004). Prior infection and passive transfer of neutralizing antibody prevent replication of severe acute respiratory syndrome coronavirus in the respiratory tract of mice. *Journal of Virology*, **78**, 3572–3577.

To, K. F., Tong, J. H., Chan, P. K., Au, F. W., Chim, S. S., Chan, K. C., Cheung, J. L., Liu, E. Y., Tse, G. M. and Lo, A. W., et al. (2004). Tissue and cellular tropism of the coronavirus associated with severe acute respiratory syndrome: an *in-situ* hybridization study of fatal cases. *Journal of Pathology*, **202**, 157–163.

Tse, G. M., To, K. F., Chan, P. K., Lo, A. W., Ng, K. C., Wu, A., Lee, N., Wong, H. C., Mak, S. M. and Chan, K. F., et al. (2004). Pulmonary pathological features in coronavirus associated severe acute respiratory syndrome (SARS). *Journal of Clinical Pathology*, **57**, 260–265.

Tu, C., Crameri, G., Kong, X., Chen, J., Sun, Y., Yu, M., Xiang, H., Xia, X., Liu, S. and Ren, T., et al. (2004). Antibodies to SARS coronavirus in civets. *Emerging Infectious Diseases*, **10**, 2244–2248.

Wang, L.-F., Shi, Z., Zhang, S., Field, H., Daszak, P. and Eaton, B. T. (2006). Review of bats and SARS. *Emerging Infectious Diseases*, **12**, 1834–1840.

Wu, D., Tu, C., Xin, C., Xuan, H., Meng, Q., Liu, Y., Yu, Y., Guan, Y., Jiang, Y. and Yin, X., et al. (2005). Civets are equally susceptible to experimental infection by two different severe acute respiratory syndrome coronavirus isolates. *Journal of Virology*, **79**, 2620–2625.

Zhao, J. M., Zhou, G. D., Sun, Y. L., Wang, S. S., Yang, J. F., Meng, E. H., Pan, D., Li, W. S., Zhou, X. S. and Wang, Y. D., et al. (2003). Clinical pathology and pathogenesis of severe acute respiratory syndrome. *Zhonghua Shi Yan He Lin Chuang Bing Du Xue Za Zhi*, **17**, 217–221.

[*Received, March 27th, 2007*
Accepted, December 26th, 2007]